



## The binding of $\beta$ -D-glucopyranosyl-thiosemicarbazone derivatives to glycogen phosphorylase: A new class of inhibitors

Kyra-Melinda Alexacou<sup>a,b</sup>, Alia-Cristina Tenchiu (Deleanu)<sup>a</sup>, Evangelia D. Chrysina<sup>a</sup>, Maria-Despoina Charavgi<sup>a</sup>, Ioannis D. Kostas<sup>a,\*</sup>, Spyros E. Zographos<sup>a</sup>, Nikos G. Oikonomakos<sup>a,†</sup>, Demetres D. Leonidas<sup>a,c,\*</sup>

<sup>a</sup> Institute of Organic and Pharmaceutical Chemistry, National Hellenic Research Foundation, 48 Vassileos Constantinou Avenue, 11635 Athens, Greece

<sup>b</sup> Department of Biology, Chemistry and Pharmacy, Freie Universität Berlin, Takustr. 3, 14195 Berlin, Germany

<sup>c</sup> Department of Biochemistry and Biotechnology, University of Thessaly, 26 Ploutonos Str., 41221 Larissa, Greece

### ARTICLE INFO

#### Article history:

Received 11 June 2010

Revised 9 September 2010

Accepted 16 September 2010

Available online 22 September 2010

#### Keywords:

Type 2 diabetes

Glycogen phosphorylase

Glucopyranosyl-thiosemicarbazones

Inhibition

X-ray crystallography

### ABSTRACT

Glycogen phosphorylase (GP) is a promising target for the treatment of type 2 diabetes. In the process of structure based drug design for GP, a group of 15 aromatic aldehyde 4-( $\beta$ -D-glucopyranosyl)thiosemicarbazones have been synthesized and evaluated as inhibitors of rabbit muscle glycogen phosphorylase b (GPb) by kinetic studies. These compounds are competitive inhibitors of GPb with respect to  $\alpha$ -D-glucose-1-phosphate with  $IC_{50}$  values ranging from 5.7 to 524.3  $\mu$ M. In order to elucidate the structural basis of their inhibition, the crystal structures of these compounds in complex with GPb at 1.95–2.23 Å resolution were determined. The complex structures reveal that the inhibitors are accommodated at the catalytic site with the glucopyranosyl moiety at approximately the same position as  $\alpha$ -D-glucose and stabilize the T conformation of the 280s loop. The thiosemicarbazone part of the studied glucosyl thiosemicarbazones possess a moiety derived from substituted benzaldehydes with  $NO_2$ , F, Cl, Br, OH, OMe,  $CF_3$ , or Me at the *ortho*-, *meta*- or *para*-position of the aromatic ring as well as a moiety derived from 4-pyridinecarboxaldehyde. These fit tightly into the  $\beta$ -pocket, a side channel from the catalytic site with no access to the bulk solvent. The differences in their inhibitory potency can be interpreted in terms of variations in the interactions of the aldehyde-derived moiety with protein residues in the  $\beta$ -pocket. In addition, 14 out of the 15 studied inhibitors were found bound at the new allosteric site of the enzyme.

© 2010 Elsevier Ltd. All rights reserved.

### 1. Introduction

Diabetes type 2 is a complex disease characterized by insulin resistance and abnormal insulin secretion. It is the most common type of diabetes. It is estimated that the number of patients suffering from type 2 diabetes will reach 300 million by the year 2025.<sup>1</sup> Glycogen phosphorylase (GP) catalyzes the first step of the intracellular degradation of glycogen, which is an important source of hepatic glucose production. Thus, inhibition of GP has emerged as a potential therapeutic strategy for type 2 diabetes.<sup>2–4</sup> GP is a dimer composed of two identical subunits associated with the

co-factor pyridoxal-5'-phosphate. It is regulated allosterically and by phosphorylation and it exists in two forms: the unphosphorylated T state GPb and the phosphorylated R state GPa.<sup>4</sup> In the last decade GP has been the target for inhibitor design<sup>5</sup> and many compounds have been reported to bind to four distinct sites, the catalytic, the allosteric, the new allosteric (or indole), and the inhibitor (or caffeine site).<sup>4</sup> The efficacy of such inhibitors on blood glucose control and hepatic glycogen balance has been confirmed from animal studies and in vitro cell biology experiments.<sup>5–7</sup>

The catalytic site of GP is buried at the centre of the monomer, where domains 1 (residues 1–484) and 2 (residues 485–842) come together. This site has been extensively investigated with glucose analogue inhibitors that bind at this site and promote the less active T state through stabilisation of the closed position of the 280s loop (residues 282–287).<sup>8</sup> On transition from T state to R state (activation of the enzyme), the 280s loop becomes disordered and displaced, opening a channel that allows a crucial residue, Arg569, to enter the catalytic site. This creates the recognition site for the substrate phosphate that also allows access of the glycogen substrate to reach the catalytic site.<sup>4</sup> Apart from the catalytic site GP has an allosteric site, which binds the allosteric activator

**Abbreviations:** GP, glycogen phosphorylase, 1,4- $\alpha$ -D-glucan:orthophosphate  $\alpha$ -glucosyltransferase (EC 2.4.1.1); GPb, rabbit muscle glycogen phosphorylase b; PLP, pyridoxal 5'-phosphate; glucose,  $\alpha$ -D-glucose; Glc-1-P,  $\alpha$ -D-glucose 1-phosphate; rmsd, root-mean-square distance.

\* Corresponding authors. Tel.: +30 210 7273878; fax: +30 210 7273831 (I.D.K.); tel.: +30 2410 565278; fax: +30 2410 565290 (D.D.L.).

E-mail addresses: [ikostas@eie.gr](mailto:ikostas@eie.gr) (I.D. Kostas), [ddleonidas@bio.uth.gr](mailto:ddleonidas@bio.uth.gr) (D.D. Leonidas).

<sup>†</sup> Deceased on August 31st 2008.

AMP, situated at the subunit–subunit interface some 30 Å from the catalytic site. There is also an inhibitor site, located on the surface of the enzyme some 12 Å from the catalytic site, which binds purine compounds, nucleosides or nucleotides. The inhibitor site obstructs the entrance to the catalytic site tunnel stabilizing the T state conformation of the enzyme. GP has also a storage site, located on the surface of the molecule, some 30 Å from the catalytic site which might serve as a region through which the mammalian enzyme is attached to glycogen particles *in vivo*.<sup>4</sup> Finally, a new allosteric site was discovered from crystallographic studies of the binding of indole-carboxamide and related synthetic counterparts.<sup>9,10</sup> The new allosteric (or indole) binding site, located inside the central cavity of the dimeric enzyme, is formed on association of the two subunits; the central cavity is partially closed at one end by residues from the cap' region (residues 47–78 from the symmetry related subunit) and  $\alpha$ 2 helices (Arg33, His34, Arg60 and Asp61 and their symmetry related equivalents) and at the other end by the  $\alpha$ 7 tower helices (residues Asn270, Glu273, Ser276 and their symmetry related equivalents).<sup>4</sup>

We have previously studied the binding of *N'*-benzoyl-*N*- $\beta$ -D-glucopyranosyl urea (Bzurea) to GPb and shown that Bzurea is a potent inhibitor of GPb displaying a  $K_i$  value of 4.6  $\mu$ M.<sup>11</sup> Structural information available from the crystal structure of the GPb-complex at 1.8 Å resolution<sup>11</sup> revealed that Bzurea, binds tightly at the catalytic site and induces significant conformational changes in the vicinity of the site. In particular the 280s loop (residues 282–287) shifts 1.3–3.7 Å ( $C\alpha$  atoms) to accommodate Bzurea. In this way the inhibitor promotes the less active T state enzyme through stabilization of the closed position of the 280s loop which blocks access of the substrate to the catalytic site. The urea and benzoyl moieties fit tightly into the so-called  $\beta$ -pocket, a side channel from the catalytic site with no access to the bulk solvent.<sup>4</sup> Furthermore, Bzurea binds at the new allosteric site of GPb, which is highly specific for indole derivatives and currently a target for the development of hypoglycaemic drugs.<sup>8</sup>

Thiosemicarbazones are a class of biochemically important compounds possessing a wide range of biological activity, and are very promising in the treatment of many diseases.<sup>12–15</sup> In a recent paper, we reported a systematic study for the synthesis and characterization of a novel class of  $\beta$ -D-glucopyranosyl-thiosemicarbazone derivatives.<sup>16</sup> Using as lead Bzurea, we have now assessed the inhibitory potential of a series of thiosemicarbazone derivatives of  $\beta$ -D-glucopyranose (Table 1) to GPb. In these compounds, the urea moiety of Bzurea is replaced by a thiosemicarbazone to (i) elongate the linker of the group that binds at the  $\beta$ -pocket of the catalytic site and (ii) to test the contribution of the carbonyl oxygen of urea interactions to the inhibitory potency. In addition, instead of the benzoyl group of Bzurea, 14 compounds possess a phenyl ring with variety of groups attached at either *ortho*, *meta* or *para*-position with respect to the thiosemicarbazone moiety while one has a pyridine. This served to investigate the ability of various groups to enhance the inhibitory potency of these thio-

semicarbazone derivatives. All compounds were found to be competitive inhibitors of GPb with respect to glucose-1-phosphate (Glc-1-P). We also report here on the crystallographic binding of these 15 derivatives to GPb, in order to provide rationalizations for their kinetic properties. Crystallographic data show that these compounds bind at the catalytic site and at the indole-carboxamide site of GPb (Fig. 1), with the exception of a molecule with an *ortho*-nitro substituted phenyl ring which was found bound only at the catalytic site. Identification of the structural determinants contributing to inhibitor binding mode at the catalytic site should provide better understanding of the mechanism of inhibition of GP, and aid the design of compounds with improved potency against GP.

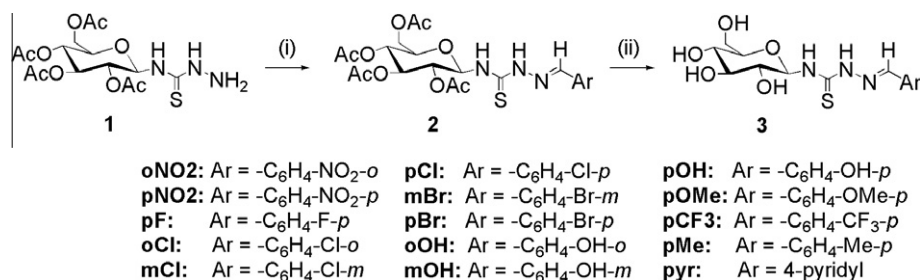
## 2. Results and discussion

### 2.1. Organic synthesis

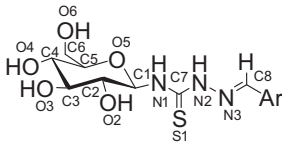
The synthesis and characterization of the aromatic aldehyde 4-( $\beta$ -D-glucopyranosyl)thiosemicarbazones **3**, outlined in Scheme 1, was achieved as recently reported by us.<sup>16</sup> Condensation of 4-(per-O-acetylated- $\beta$ -D-glucopyranosyl)thiosemicarbazide **1** with a number of aldehydes according to a known procedure,<sup>17,18</sup> afforded aldehyde 4-(per-O-acetylated- $\beta$ -D-glucopyranosyl)thiosemicarbazones **2**, the acetyl protective groups of which were removed by the Zemplén method<sup>19</sup> in absolute methanol in the presence of sodium methoxide. The spectral data indicate the  $\beta$  configuration, and the *E* configuration pertaining to the stereochemistry of the C=N bond.<sup>16</sup> Compounds **3pF**, **3mBr** and **3pBr** are new members of this class of bioactive molecules.

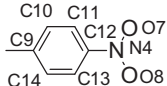
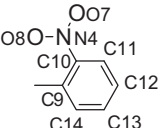
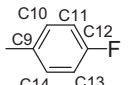
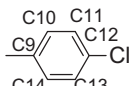
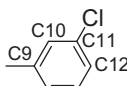
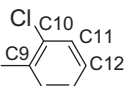
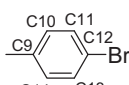
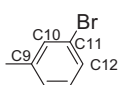
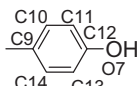
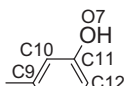
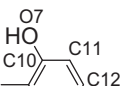
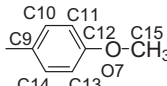
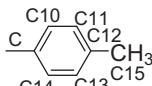
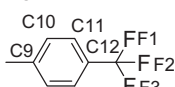
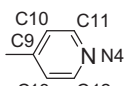
### 2.2. Enzyme kinetics

The inhibitory efficiency of the thiosemicarbazone derivatives was tested in kinetic experiments with rabbit muscle glycogen phosphorylase b (GPb) and their inhibition constants are presented in Table 1. All compounds displayed competitive inhibition with respect to the substrate Glc-1-P, at constant concentrations of glycogen (0.2% w/v) and AMP (1 mM) with  $IC_{50}$  values at the  $\mu$ M range. The most potent compound is **3pF**, with a fluorine atom at the *para*-position of the aromatic ring with  $IC_{50} = 5.7 \mu$ M while the least potent is compound **3pCF3** ( $IC_{50} = 524.3 \mu$ M), with a  $-CF_3$  group at the same position. Comparison of the ligands with a *para* substitution (column 1, Table 1) indicates that the inhibitory potency decreases with the increase in bulkiness of the substituent at this position. This is also evident when comparing the potency of compounds **3pOMe** (methoxy) and **3pMe** (methyl), which have  $IC_{50}$  values of 406.5  $\mu$ M and 192.4  $\mu$ M, respectively or when comparing the potency of **3pF** with that of **3pMe**. The only exception to this observation is the nitro compound **3pNO2**, which is among the best inhibitors of the enzyme. This exception indicates that the chemical properties of the substituent also affect significantly the



**Scheme 1.** Reagents and conditions: (i)  $ArCH=O$ , EtOH or MeOH, cat. AcOH, reflux; (ii) NaOMe, MeOH, rt. For compounds **2oNO2**, **2pNO2**, **2oCl**, **2mCl**, **2pCl**, **2oOH**, **2mOH**, **2pOH**, **2pOMe**, **2pCF3**, **2pMe**, **2pyr** and **3oNO2**, **3pNO2**, **3oCl**, **3mCl**, **3pCl**, **3oOH**, **3mOH**, **3pOH**, **3pOMe**, **3pCF3**, **3pMe**, **3pyr** see Ref. 16.

**Table 1**Inhibitory efficiency of the thiosemicarbazone derivatives of  $\beta$ -D-glucopyranose and the atom numbering scheme used in crystal structures


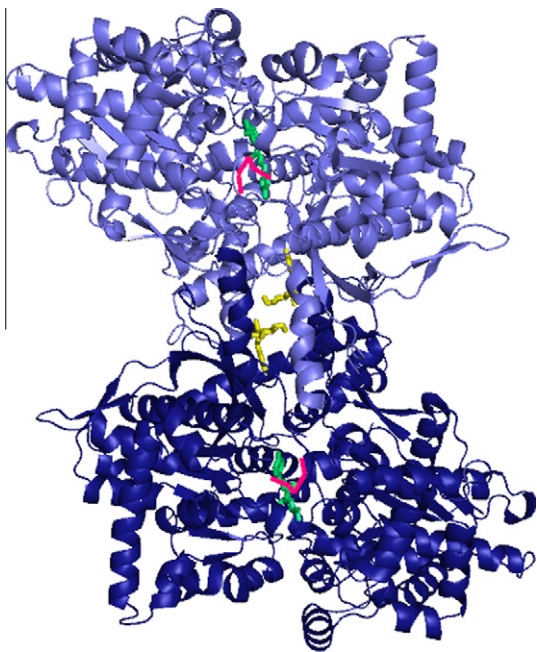
	Ar group	IC <sub>50</sub> (μM)		Ar group	IC <sub>50</sub> (μM)		Ar group	IC <sub>50</sub> (μM)
<b>3pNO2</b>		25.7 ± 0.9				<b>3oNO2</b>		484.2 ± 23.3
<b>3pF</b>		5.7 ± 0.4						
<b>3pCl</b>		28.3 ± 1.7	<b>3mCl</b>		23.2 ± 0.5	<b>3oCl</b>		370.0 ± 9.7
<b>3pBr</b>		93.2 ± 5.1	<b>3mBr</b>		50.4 ± 1.9			
<b>3pOH</b>		340.5 ± 21.7	<b>3mOH</b>		180.0 ± 7.8	<b>3oOH</b>		26.6 ± 3.3
<b>3pOMe</b>		406.5 ± 40.6						
<b>3pMe</b>		192.4 ± 5.8						
<b>3pCF3</b>		524.3 ± 11.4						
<b>3pyr</b>		200.0 ± 17.0						

potency of the ligand. Comparison of the position (*ortho*, *meta* or *para*) of the substituent at the phenyl ring reveals that within the compounds with chlorine atom (**3pCl**, **3mCl**, and **3oCl**) the order of potency is *para*  $\approx$  *meta* > *ortho* while for those with a hydroxyl group (**3oOH**, **3mOH**, and **3pOH**) is *ortho* > *meta* > *para*. The potency of compounds **3pBr** and **3mBr** with a bromine atom at *para* and *meta* position does not differ much (IC<sub>50</sub> values 93.2 μM and 50.4 μM) while **3oNO2** and **3pNO2** with a nitro group at *ortho* and *para*-position, show large differences in their potency with IC<sub>50</sub> values of 484.2 μM and 25.7 μM, respectively. Therefore a general pattern with respect to the position of the substituent (i.e., *para* is better than *meta*) is not evident from the kinetics results. However, it seems that the inhibitory potency of the compounds depends mostly on the chemical and physical properties (size, charge, polarizability, etc) of the decorating groups of the phenyl ring. Thus, for halogens the best position is the *meta*, for the nitro group the *para* and for the hydroxyl the *ortho* position.

Compound **3pF** (IC<sub>50</sub> = 5.7 μM) is almost equipotent with Bzurea (*K<sub>i</sub>* = 4.6 μM),<sup>11</sup> while the rest of the inhibitors are poor inhibitors compared to their lead molecule (Bzurea). However, compounds **3pNO2**, **3mCl**, **3pCl**, **3mBr** and **3oOH** are still considered as potent inhibitors with IC<sub>50</sub> values less than 50 μM and could be exploited as improved leads for further optimization.

### 2.3. Structural studies

In order to elucidate the structural basis of inhibition we have determined the crystal structure of GPb in complex with each of the 15 compounds presented in Table 1. A summary of the data processing and refinement statistics for the inhibitor complex structures is given in Supplementary data Tables S1–S3. The 2F<sub>o</sub> – F<sub>c</sub> and F<sub>o</sub> – F<sub>c</sub> Fourier electron density maps calculated using the coordinates of the native structure indicated that all compounds except **3oNO2** were bound at both the catalytic site and



**Figure 1.** A schematic diagram of the GPb dimeric molecule viewed down the molecular dyad. One subunit is colored in dark blue and the other in light blue. The catalytic and the new allosteric site are marked by bound compound **3pF** (in green and yellow, respectively). Compound **3pF**, on binding to the catalytic site, promotes the less active T state through stabilization of the closed position of the 280 s loop (shown in pink and thicker) which blocks access for the substrate (glycogen) to the catalytic site.

at the new allosteric site. **3oNO2** was found bound only at the catalytic site. Electron density maps clearly defined the position of each atom of the inhibitors within the catalytic and the new allosteric site. In crystallographic experiments with a soak of 1 mM of each inhibitor for 3.5 h, electron density maps suggested strong binding to the catalytic site, but partial occupancy of the new allosteric site by the ligand. It seems therefore that the new allosteric site is not the primary binding site for these inhibitors. A similar situation has been also observed with Bzurea.<sup>11</sup>

The structural results show that all inhibitors are bound with essentially no disturbance of the overall protein structure. The superimposition of the structures of native GPb and the GPb–inhibitor complexes over well defined residues (18–249, 262–312, 326–829) gave rmsd values 0.2–0.4 Å (C $\alpha$  positions). However, upon binding to the catalytic site compounds **3pBr**, **3pCl**, **3pCF3**, **3oOH**, **3pOMe** and **3pMe** trigger a significant shift of the 280s loop with concomitant changes in the adjacent imidazole of His571. Thus, the range of the rmsd values between the structures of GPb–inhibitor and native GPb for main chain atoms is for residues Asn282 (0.4–0.7 Å), Asp283, (0.7–1.0 Å), Asn284 (1.1–1.8 Å), Phe285 (0.8–0.9 Å), Phe286 (0.6–0.7 Å), and Glu287 (0.3–0.4 Å). In the native structure, the side chain atom NE2 of His571 forms a hydrogen bond with the side chain atom OD2 of Asp283. In the complex structures with compounds **3pBr**, **3pCl**, **3pCF3**, **3oOH**, **3pOMe** and **3pMe** the side chain of His571 is rotated ( $\chi_1 \approx 20^\circ$ ) to maintain this hydrogen bond with the side chain of Asp283 at the new position. Furthermore, the conformational change of the 280s loop results in Asn284 being sandwiched between the side chains of Phe285 and Tyr613. These phenyl rings are the key components of the inhibitor site of GPb, a site that binds caffeine and a number of other fused ring compounds.<sup>4,5,8</sup> The insertion of Asn284 leads to the destruction of this site. This mimics the T to R allosteric transition, which also involves movement of the 280s loop.<sup>20</sup> However, a structural comparison between the present GPb complexes and maltodextrin phosphorylase<sup>21,22</sup>

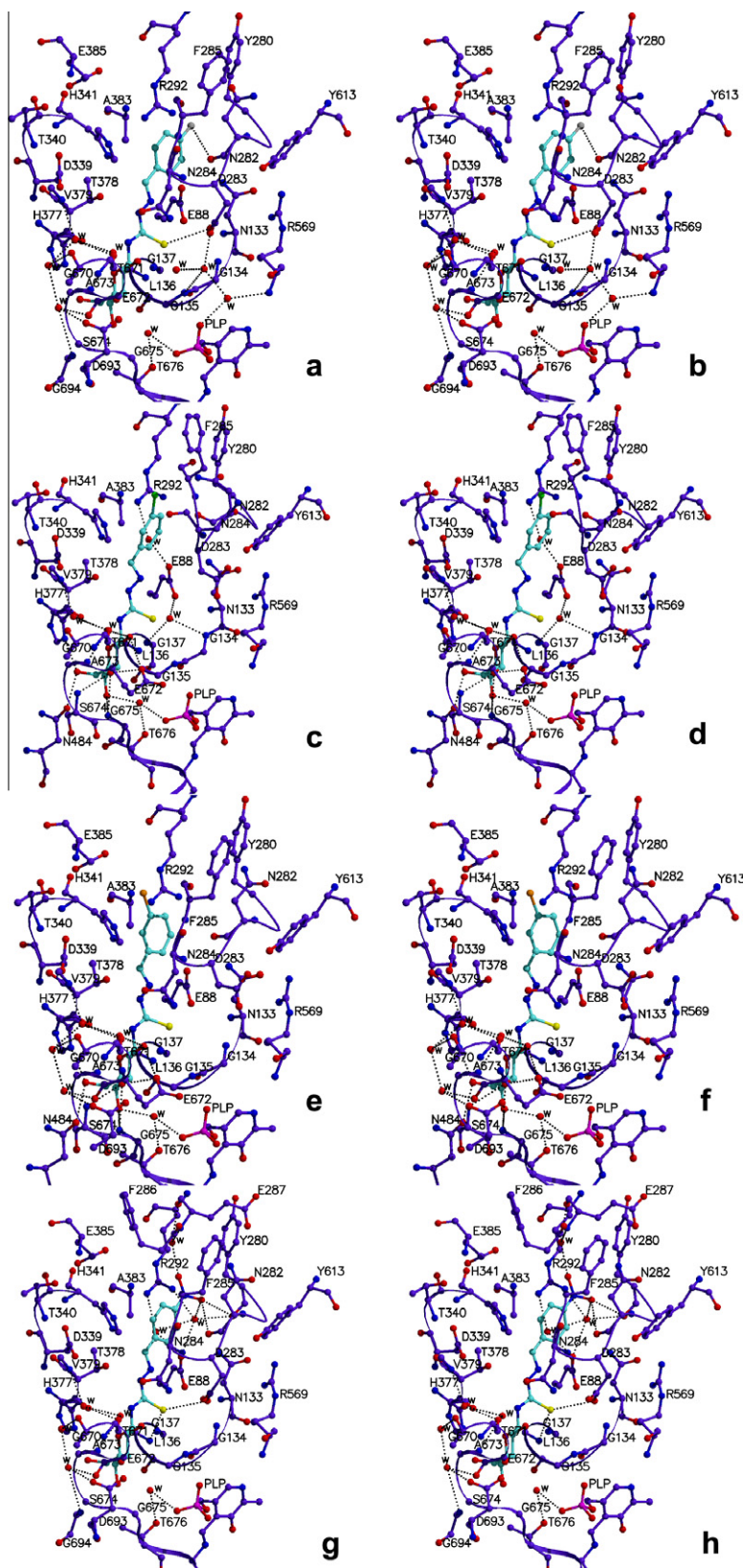
where the 280s loop is held in an open conformation (in the R state GPb the 280s loop is disordered and its position ambiguous<sup>23</sup>) in the vicinity of the catalytic site has shown that the shifts of the 280s loop are not in the direction of the T to R allosteric transition. In addition, the new position of the 280s loop imposed by the binding of the present inhibitors still obstructs the entrance to the catalytic site of GPb and therefore all fifteen inhibitors can be classified as T state inhibitors. The mode of binding and the interactions that the glucopyranose moiety of all fifteen compounds makes with GPb residues at the catalytic site are almost identical with that of  $\alpha$ -D-glucose.<sup>24,25</sup> The benzaldehyde-derived thiosemicarbazone moiety is accommodated at the  $\beta$ -pocket of the catalytic site forming mainly van der Waals interactions with the protein. The sulfur group of thiosemicarbazone is hydrogen-bonded either directly to Asp283 OD1 (compounds **3pF**, **3oCl** and **3pOH**) or Leu136N (compounds **3pBr**, **3pCl**, **3pCF3**, **3pOMe** and **3pMe**), or to both (compounds **3pNO2** and **3pyr**) or through a water molecule (compounds **3mBr**, **3mCl**, **3oNO2**, **3oOH**, and **3mOH**) to the side chain of Asp283. Apart from these interactions the thiosemicarbazone moiety is not involved in any other hydrogen bond interactions with neighbouring residues. The hydrogen bond between N1 of N-acetyl- $\beta$ -D-glucopyranosylamine (NAG) and carbonyl O of His377, an interaction that has been observed in all  $\beta$ -D-glucopyranosylamine analogues<sup>4,8</sup> has not been observed in this complex similarly to the Bzurea complex.<sup>11</sup> At the new allosteric site the glucopyranose moiety is engaged in hydrogen bond interactions with the side chain atoms of Glu190, and the main chain nitrogen of Ala192, while four water molecules mediate hydrogen bonds with side chain atoms of His57, Arg60, Asn187, and Tyr226. In addition, N1 from the thiosemicarbazone moiety forms a hydrogen bond with the carbonyl oxygen of Glu190 while N2 and N3 form hydrogen bonds with the side chain of Arg160. The interactions between **3pF**, **3mBr**, **3mCl** and **3pNO2** and the protein are shown in Figure 2.

The glucopyranosyl-thiosemicarbazone derivatives studied have a benzaldehyde-derived group attached at the C8 position (Table 1), which has either a –Br or a –Cl or a –OH, or a –Me, or a –OMe or a –NO<sub>2</sub>, or a –F at *ortho*, *para* or *meta* positions or instead of a benzaldehyde-derived group there is a pyridinecarboxaldehyde-derived moiety. Since the conformation (Fig. 3) and the protein–ligand interactions pattern of the glucopyranosyl ring and the thiosemicarbazone linker of the derivatives upon binding to the catalytic site is very similar, and the same applies for the inhibitors bound at the new allosteric site, we describe below in more detail the interactions of the phenyl or pyridyl moiety of compounds with GPb in groups according to the substituent group of the aromatic ring of the inhibitors.

### 2.3.1. The nitro group

Inhibitors **3oNO2** and **3pNO2**, 2- and 4-nitro-benzaldehyde 4-( $\beta$ -D-glucopyranosyl) thiosemicarbazone upon binding to the catalytic site of GPb take part in 11 and 14 hydrogen bond interactions with the protein, while they exploit 114 and 129 van der Waals interactions with GPb residues, respectively (Fig. 2). Interestingly structural comparison of the complexes with the native enzyme reveals that the binding of the two inhibitors does not cause any significant conformational changes including the 280s loop. The nitro group in compound **3oNO2** participates in a hydrogen bond interaction with the side chain of Glu88 (Table 2) and water mediated hydrogen bonds with the main chain nitrogen of Gly134 and Gly137. In compound **3pNO2** the nitro group is involved in hydrogen bond interactions with the carbonyl oxygen of Tyr280 and Asn282 (Table 2) and a water mediated hydrogen bond with the carbonyl oxygen of Glu287 (Fig. 2). Kinetic studies revealed that inhibitor **3pNO2** (*para*-position) is almost 19 times more potent than **3oNO2** (*ortho* position). This

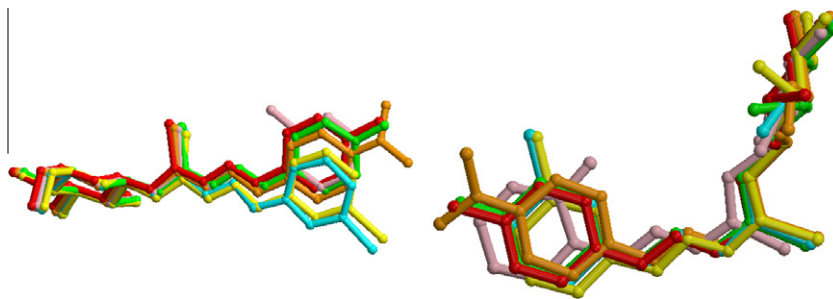




**Figure 2.** Schematic diagram of the molecular interactions between GpB and inhibitors **3pF**, **3mBr**, **3mCl**, and **3pNO2** when bound at the catalytic site (a, c, e, g) and at the new allosteric site of GpB (b, d, f, h). The side chains of protein residues involved in ligand binding are shown as ball-and-stick models. Hydrogen bond interactions between the inhibitors, protein residues and water molecules (w) are represented as dotted lines.

difference in their potency can be attributed (i) to the three additional hydrogen bond interactions of **3pNO2** with respect to those of **3oNO2**, and (ii) to the hydrogen bonds of atom O7 of the nitro

group of **3pNO2** with the main chain oxygen atoms of Tyr280 and Asn282 from the 280s loop (unlike the nitro group of **3oNO2** which does not form any interactions with residues of the 280s



**Figure 3.** Structural comparisons of the ligand molecules when bound at the catalytic (left) and at the new allosteric site (right) of GPb are shown in color; **3pF** green, **3mBr** yellow, **3mCl** cyan, **3pNO2** orange, **3oOH** pink, and **3pMe** red.

**Table 2**  
Interactions of the aryl ring substituent of the inhibitors with GPb residues at the catalytic site

Code	Hydrogen/halogen bonds	No of Van der Waals interactions	Code	Hydrogen/halogen bonds	No of Van der Waals interactions	Code	Hydrogen/halogen bonds	No of Van der Waals interactions
<b>3pNO2</b>	Tyr280 O; Asn282 O	13				<b>3oNO2</b>	Glu88 OE1	15
<b>3pF</b>	Asn282 O	6				<b>3oCl</b>	Phe285 N	6
<b>3pCl</b>	—	11	<b>3mCl</b>	Phe285 O; Ala383 O	4			
<b>3pBr</b>	Asn282 OD1	10	<b>3mBr</b>	Phe285 O	7			
<b>3pOH</b>	Asn282 O	0	<b>3mOH</b>	Asn282 O; Ala383 O	2	<b>3oOH</b>	Asp283 O	6
<b>3pOMe</b>	—	15						
<b>3pMe</b>	—	8						
<b>3pCF3</b>	Tyr280 O; Asn282 O, OD1; Arg292 NH1, NH2	27						
<b>3pyr</b>	Asp339 OD2; Ala383 O	3						

loop) that lead to further stabilization of its closed conformation.

Upon binding to the new allosteric site of GPb, inhibitor **3pNO2** forms three direct and six water mediated hydrogen bonds and 79 van der Waals interactions with GPb residues (Fig. 2). Structural comparison with Bzurea bound at this site revealed that the glucopyranose moiety shifts to opposite directions by approximately 93° with respect to the backbone. Inhibitor **3oNO2** was not found bound at the new allosteric site.

### 2.3.2. The halogen group

The conformation of the halogen inhibitors when bound at the catalytic site of GPb are very similar (Fig. 3). **3pF** upon binding at the catalytic site of GPb forms 10 hydrogen bonds and 101 van der Waals interactions (Fig. 2), while inhibitor **3pCF3** forms 11 hydrogen bonds and 95 van der Waals interactions with protein residues. Compound **3pCl** forms 9 hydrogen bonds, and 103 van der Waals interactions with the protein residues at the catalytic site, respectively while **3pBr** participates in 9 hydrogen-bonding interactions and 100 van der Waals interactions with residues of GPb at the same site.

Fluorine is a poorer hydrogen bond acceptor than oxygen (it cannot act as a donor)<sup>26</sup> and it affects significantly the hydrogen-bonding interactions between a ligand and residues of the catalytic site of GPb<sup>27</sup> that cannot donate a proton. In the **3pF** complex, fluorine forms a halogen bond<sup>28</sup> with Asn282 O whereas the fluorine atoms of the trifluoromethyl group of **3pCF3** engage in hydrogen bond interactions with the side chain atoms of Arg292, the main chain oxygen and the side chain OD1 of Asn282, and a water mediated interaction with the side chain of Glu88. In **3pCl** the chloride group is involved only in 11 van der Waals interactions while in **3pBr** bromine is involved in hydrogen bond interactions with Asn282 OD1 in addition to 10 van der Waals interactions (Table 2). Upon binding to the

catalytic site of GPb, compounds **3mCl**, **3mBr** and **3oCl**, form 8, 8, and 9 hydrogen bonds, and 97, 86 and 100 van der Waals interactions with the protein residues, respectively (Fig. 2). The chloride group of **3mCl** forms two halogen bonds with the carbonyl oxygen atoms of Phe285 and Ala383 O and the chloro-phenyl ring engages in 4 van der Waals interactions. The bromide group of compound **3mBr** engages in a halogen bond interaction<sup>29</sup> with the carbonyl oxygen of Phe285 while the bromo-phenyl ring takes part in 7 van der Waals interactions with protein residues (Table 2). In the **3oCl** complex the chloride group forms a hydrogen bond with the main chain nitrogen of Phe285 and the chloro-phenyl ring participates in 6 van der Waals interactions with GPb residues (Table 2).

The most interesting observation of the binding of the halogen compounds is that the binding of **3pCF3**, **3pCl**, and **3pBr** causes a significant conformational change of the GPb residues of the 280s loop and on average the C $\alpha$  atoms of residues 282–287 are shifted by 1.0 Å from their positions at the native structure. This conformational change is less profound in the **3pF**, **3mCl**, and **3mBr** complexes where the average shift of all atoms of residues 282–287 is 0.3 Å while in the **3oCl** complex this was not observed. Interestingly, the trifluoromethyl derivative triggers significant conformational changes to the 280s loop whereas the effect of the binding of the fluoro-compound is less profound. Therefore, it seems that the *para* halogen substituents trigger a most significant conformational change than those at the *meta* or *ortho* position. The exception of **3pF** might be attributed to the smaller size of the fluoride group as compared to those of the trifluoromethyl, chloride or bromide group.

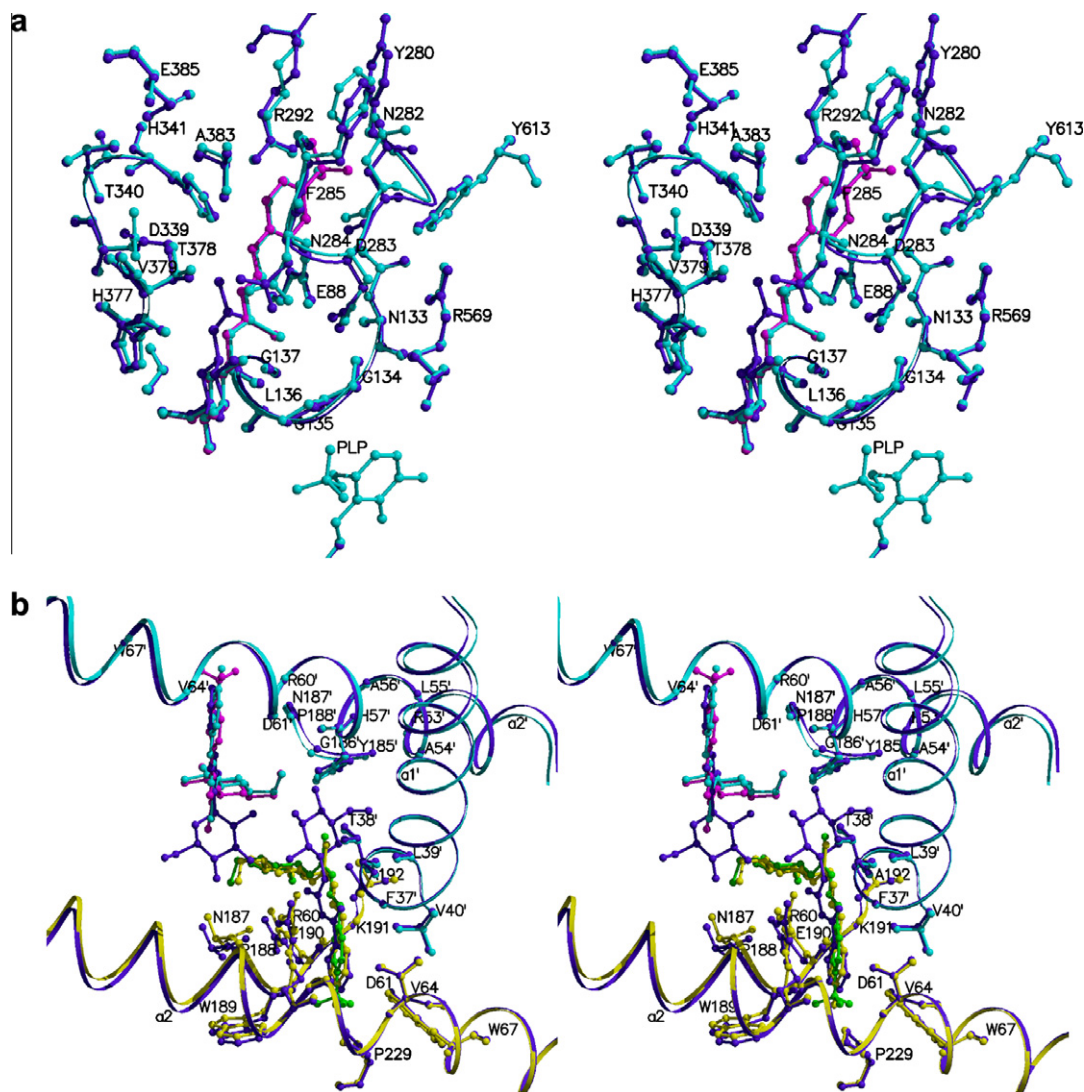
Kinetic studies revealed that compound **3pF** is the most potent of all 15 compounds presented here, almost 92 times more potent than compound **3pCF3** and equipotent to Bzurea.<sup>11</sup> Structural comparison of the GPb–**3pF** complex with the GPb–Bzurea complex at the catalytic site (Fig. 4a) showed that the two inhibitors bind in a

similar manner and this provides a structural basis for their equipotency. Therefore it seems that replacement of the urea moiety with a thiosemicarbazone does not affect the potency of the inhibitor since Bzurea and **3pF** are equipotent.

Kinetic studies revealed that **3pCl** and **3mCl**, (*para* and *meta* position) have a significant better inhibitory effect on GPb, than the **3oCl** (*ortho*) derivative with IC<sub>50</sub> values 16 and 13 times lower, respectively. The binding position of the chloro-phenyl ring is different in the three compounds. Its position in compound **3mCl** is 1.8 Å apart from its position in compounds **3oCl** and **3pCl**, and the angle between the planes of the benzyl ring in the two latter compounds is ~20°. The chloride group is engaged in halogen bond interactions with the carbonyl oxygen of Phe285 and Ala383 in compound **3mCl** and with the main chain nitrogen of Phe285 in compound **3oCl**, while in compound **3pCl** is involved only in van der Waals interactions (Table 2). However, the most interesting observation of the binding of the chloro-compounds is that compounds **3mCl** and **3pCl** induce the 280s loop conformational change described above whereas compound **3oCl** does not. This conformational change and the stabilization of the 280s loop seem to form the structural basis for the much higher potency of compounds **3pCl** and **3mCl** with respect to **3oCl**.

Kinetic experiments indicated that inhibitors **3pBr** and **3mBr** are almost equipotent (Table 1) and this is consistent with structural studies that show that both inhibitors bind very similarly to the catalytic site of GPb engaging in approximately the same number of interactions with protein residues (Table 2). Furthermore, on binding both compounds **3pBr** and **3mBr** displace five water molecules from the active site of the unliganded structure.

Upon binding to the new allosteric site of GPb, inhibitors **3pF** and **3pCF3** form 4 hydrogen bonds each and 111 and 77 van der Waals interactions, respectively (Fig. 2). The fluoro and fluoromethyl groups do not engage in any hydrogen bond interactions with protein residues. Structural comparison with the Bzurea binding revealed that the β-D-glucopyranose moiety in the two ligands is shifted to an opposite direction (Fig. 4b). Upon binding to the new allosteric site of GPb, compounds **3oCl**, **3mCl**, and **3pCl** form three hydrogen bonds each and exploit 64, 79, 85 van der Waals interactions, respectively (Fig. 2). A structural comparison with Bzurea which also binds at the same site<sup>11</sup> revealed that the glucopyranose moiety once again shifts to opposite directions by approximately 93° with respect to the backbone. The binding of **3oCl**, **3mCl**, and **3pCl** at the new allosteric site does not promote any significant conformational changes apart from the shift of



**Figure 4.** (a) Stereo diagrams of the structural comparison between GPb in complex with **3pF** (cyan) and *N'*-benzoyl-*N*-β-D-glucopyranosyl urea<sup>11</sup> (magenta) at the catalytic site of GPb and (b) in the vicinity of the new allosteric site (*N'*-benzoyl-*N*-β-D-glucopyranosyl urea-GPb complex, magenta) and GPb-**3pCF3** complex (subunit 1, green and subunit 2 magenta).



the side chain of Arg60 which has been observed for all compounds that bind to this site. Inhibitors **3mBr** and **3pBr** were also found bound at the new allosteric site. Compound **3mBr** is bound at the new allosteric site with two alternative conformations in which the orientation of the bromo-benzyl moiety differs by 180°. Compound **3pBr** displays only one conformation at this site and both **3mBr** and **3pBr** form 7 hydrogen bonds and 34 van der Waals interactions with protein residues (Fig. 2). The most significant conformational change at this site upon binding of these inhibitors is the shift of the side chain of Arg60 by ~2.0 Å from its position at the native GPb structure, which is probably due to stereochemical impediments imposed by the inhibitor molecule and has also been observed upon binding of Bzurea to the same site. A structural comparison with the binding of Bzurea at this site<sup>11</sup> revealed only minor conformational changes.

### 2.3.3. The hydroxyl group

The 2-, 3-, and 4-hydroxy-benzaldehyde 4-( $\beta$ -D-glucopyranosyl)thiosemicarbazones (**3oOH**, **3mOH** and **3pOH**) were found bound at the catalytic and the new allosteric site. The conformation of the three compounds upon binding at the catalytic site differs. Thus, in compound **3oOH** the torsion angle C8–N3–N2–C7 is 180° so that the conformation about the N2–N3 bond is in *trans* geometry while in compounds **3mOH** and **3pOH** it is –180° (for atom numbering, see in Table 1). In addition, the hydroxyphenyl ring is coplanar with the thiosemicarbazone linker in compounds **3oOH** and **3pOH** whereas in **3mOH** is inclined by ~20°.

Upon binding to the catalytic site of GPb, inhibitors **3oOH**, **3mOH**, and **3pOH** form 15, 15 and 13 hydrogen bonds, and exploit 109, 125, and 97 van der Waals interactions, respectively (Fig. 5). The binding mode of the hydroxyphenyl group differs between the three inhibitors. The hydroxyphenyl group is bound deep in the  $\beta$ -pocket involved in van der Waals interactions with protein residues dominated by polar-non polar contacts with Glu88, Asn282, Asp283 Phe285, Arg292 and His341. The binding of **3oOH** and **3pOH** but not **3mOH** triggers significant shifts of the main chain atoms from their position in the native GPb structure. The major rmsd values of the main chain atoms are for residues Asn282 (0.7 Å), Asp283 (0.7 Å), Asn284 (1.1 Å), Phe285 (0.9 Å), and Phe286 (0.6 Å). In the **3pOH** complex the hydroxyl group is hydrogen-bonded with the carbonyl oxygen of Asn282 and it is not involved in any van der Waals interactions (Table 2). Compound **3mOH** displays two alternative conformations for the hydroxyphenyl group 180° apart and the hydroxyl group takes part in hydrogen bond interactions with either the carbonyl oxygen of Ala383 and water mediated interactions with side chain atoms of Glu88 and Arg292 or the carbonyl oxygen of Asn282 (Fig. 5, Table 2). The hydroxyl group in compound **3oOH** forms a hydrogen bond with the carbonyl oxygen of Asp283 (Table 2).

Kinetic studies revealed that **3oOH** (*ortho* position) has the best inhibitory effect on GPb with an IC<sub>50</sub> value of 26.6  $\mu$ M, while inhibitors **3mOH** and **3pOH** (*meta* and *para*-position) are less potent with IC<sub>50</sub> values of 180  $\mu$ M and 340.5  $\mu$ M, respectively. This difference in their inhibitory potency might be attributed to the number of the van der Waals interactions of the hydroxyl group with GPb residues in each inhibitor complex (Table 2). Thus, **3oOH** which displays 6 interactions is more potent than **3mOH** (2 interactions) which in turn is more potent than **3pOH** (no interactions).

On binding to the new allosteric site all three inhibitors have similar conformation which differs significantly from that observed in the catalytic site. Thus, the torsion angle C9–C8–N1–C1 is –177° and 23° in the new allosteric site. As a result the hydroxyphenyl ring and the glucopyranose ring of the bound inhibitors are not in line as in the catalytic site but inclined by approximately 30°. However, in both the catalytic and the new allosteric site the hydroxyphenyl ring is coplanar to the plane of the thiosemicar-

bazone moiety. On binding to the new allosteric site of GPb, the inhibitors make a total of four hydrogen bonds and exploit 66 van der Waals interactions. The hydroxyphenyl ring is only involved in van der Waals interactions mainly with Arg60, Val64 and Val40' from the symmetry related protein subunit.

### 2.3.4. The methoxy/methyl group

The two inhibitors, 4-methoxy-benzaldehyde 4-( $\beta$ -D-glucopyranosyl)thiosemicarbazone (**3pOMe**) and the 4-methyl analogue (**3pMe**) bind at the catalytic site of GPb in a very similar manner and conformation. Upon binding to the catalytic site of GPb, each one form nine hydrogen bonds with protein residues and they exploit 107 and 101 van der Waals interactions with GPb residues, respectively (Fig. 5). Upon binding, both inhibitors induce significant conformational changes to residues of the 280s loop and the largest shifts occur in residues Asp283 (1.0 Å at C $\alpha$  positions) and Asn284 (1.7 Å at C $\alpha$  positions). The methyl group of **3pMe** engages in 8 van der Waals interactions with GPb residues whereas the methoxy group of **3pOMe** in 15 (Table 2). The methyl derivative is almost two times more potent than the methoxy one and this cannot be explained from the structural point of view.

Upon binding to the new allosteric site of GPb, inhibitors **3pOMe** and **3pMe** form three hydrogen bonds each and 79 and 81 van der Waals interactions, respectively. No other profound conformational changes were noted in the protein environment. Comparison with Bzurea shows that the thiosemicarbazone moiety is 180° rotated with respect to the urea moiety, whereas the positions of the aromatic rings of the three inhibitors superimpose rather well. As a result the glucopyranose moiety is pointing in opposite directions in the **3pOMe**, **3pMe** and Bzurea complexes. In addition, in inhibitors **3pOMe** and **3pMe** the aryl ring is coplanar to the thiosemicarbazone moiety whereas in Bzurea is inclined by 30°.

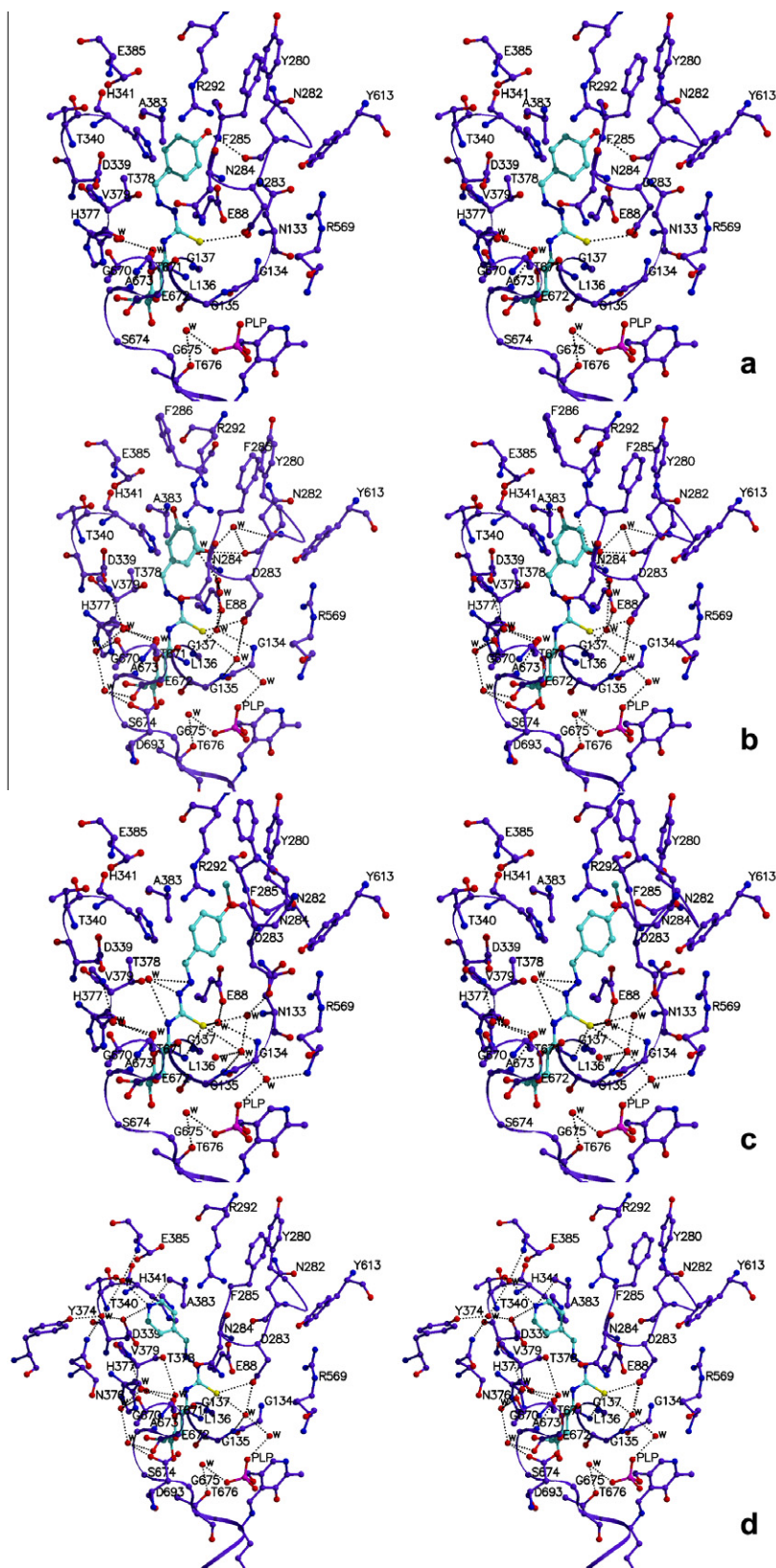
### 2.3.5. The pyridine group

The binding of 4-pyridinecarboxaldehyde 4-( $\beta$ -D-glucopyranosyl)thiosemicarbazone (**3pyr**) to the catalytic and to the new allosteric site of GPb is not accompanied by any significant conformational changes of the enzyme including the 280s loop. Inhibitor **3pyr** forms 14 and 4 hydrogen bonds, and 113 and 80 van der Waals interactions at the catalytic and the new allosteric site of GPb, respectively. Structural comparison of the **3pyr** complex with the GPb–Bzurea complex<sup>11</sup> but also with the other 14 GPb–inhibitor complexes presented here, reveals that the aromatic ring of **3pyr** is positioned at a different location compared to the rest of the inhibitors studied. Thus, the N2–N3 bond is rotated by 180° and as a result the pyridine is bound in a new position within the  $\beta$ -pocket (shifts of 3.3 Å in atom C9 and 7.3 Å in atoms N4–C12 between **3pF** and **3pyr**). In this new location the pyridine is engaged in hydrogen bond interactions with OD2 of Asp339 and the carbonyl oxygen of Ala383 and water mediated hydrogen bonds with Thr340 OG1 and Glu385N (Fig. 5). Furthermore it is involved in van der Waals interactions with atoms from residues Asp339, His341, Thr378, and Ala383. In the new allosteric site, **3pyr** binds in a similar structural mode with the rest of the 14 inhibitors presented here.

## 2.4. Conclusions

The synthesis and characterization of 15  $\beta$ -D-glucopyranosyl-thiosemicarbazones (three of which are new compounds), is reported. These have been studied with kinetic and X-ray crystallography studies for binding to GPb. These inhibitors were found to be competitive inhibitors of the enzyme with respect to Glc-1-P and they all bind to the active site by anchoring their  $\beta$ -D-glucopyranose moiety at the  $\alpha$ -D-glucose binding site and the





**Figure 5.** Stereo diagrams of the molecular interactions between Gpb and inhibitors **3pOH** (a), **3mOH** (b), **3pOMe** (c), and **3pyr** (d) when bound at the catalytic site. The side chains of protein residues involved in ligand binding are shown as ball-and-stick models. Hydrogen bond interactions between the inhibitors, protein residues and water molecules (w) are represented as dotted lines.

thiosemicarbazone moiety at the hydrophobic  $\beta$ -pocket of the active site. In addition, these inhibitors, with the exception of **3oNO2**, were also found bound at the new allosteric site of Gpb.

Binding at this site does not promote any significant conformational changes except for small shifts in the residues in the vicinity of the inhibitor (namely Arg60, Val64, Trp189 and Lys191), which

undergo conformational changes in order to accommodate the ligand. However, it should be noted that the orientation of the aromatic group is maintained as observed previously in other compounds bound at this site.<sup>8</sup>

Comparing the binding of each compound at the catalytic site, it is interesting to see that there is a pattern emerging based on the electronegativity of the directing groups. Between the three compounds with the –Cl substituent, the one in the *ortho* position of the aromatic ring causes a moderate shift of the 280s loop upon binding. The one in the *meta* position causes a significant shift in the 280s loop, while the one in the *para*-position causes a major shift in the 280s loop. However, between the three compounds with the –OH substituent the opposite effect is observed. The substituent in the *ortho* position of the aromatic ring causes the biggest shift of the 280s loop and the strongest destabilization of the protein. In the case of the –Br substituent the effect of a significant shift of the 280s loop is the same in both the *meta* and *para*-positions of the aromatic ring. In addition, there is a similarity between the –OCH<sub>3</sub> and –CH<sub>3</sub> substituents. Both cause a significant shift of the 280s loop as mentioned above. Interestingly, the binding of the inhibitors with the –NO<sub>2</sub> triggers a negligible shift of the 280s loop. Finally, is it interesting to add that among all these compounds, only **3oOH**, with the –OH substituent in the *ortho* position, changes the direction of the phenyl ring of Phe285 completely, compared to all the other cases where it is simply shifted. Out of the three inhibitors with the –OH substituent **3oOH** also causes the biggest shift and destabilization of the 280s loop. It also has the lowest K<sub>i</sub> value between the three. These observations will be of value in the design of further potent and specific inhibitors of the enzyme.

In conclusion, this study provides evidence that thiosemicarbazone derivatives of β-D-glucopyranose are potent inhibitors of glycogen phosphorylase with IC<sub>50</sub> values in the low μM range (the best inhibitor **3pF** showed an IC<sub>50</sub> of 5.7 μM) and could bind tightly at both the catalytic and new allosteric site of GPb as indicated by the high resolution structures of GPb determined in complex with 15 aromatic substituted thiosemicarbazone derivatives of β-D-glucopyranose.

### 3. Experimental section

#### 3.1. Organic synthesis

##### 3.1.1. General

4-(2,3,4,6-Tetra-O-acetyl-β-D-glucopyranosyl)thiosemicarbazide (**1**)<sup>17</sup> was synthesized by treatment of (2,3,4,6-tetra-O-acetyl-β-D-glucopyranosyl)isothiocyanate<sup>30</sup> (prepared by the reaction of potassium thiocyanate with (per-O-acetylated-α-D-glucopyranosyl)bromide;<sup>31</sup> the latter compound was prepared from D-glucose pentaacetate) with dry hydrazine in ethanol. D-Glucose pentaacetate and aldehydes were commercially available. All reactions were carried out under an argon atmosphere with purified and dry reagents and solvents. Column chromatography was performed using silica gel and TLC on Kieselgel 60 F<sub>254</sub> plates; the plates were visualized under UV light or by gentle heating after spraying with an ethanolic solution (5% H<sub>2</sub>SO<sub>4</sub>). Optical rotations were measured on a Perkin–Elmer polarimeter at room temperature. Melting points were measured on a Nikon 50i Pol microscope equipped with a Linkam THMS600 hot stage and a TMS94 temperature controller or on a Büchi melting point apparatus, and were not corrected. IR spectra were recorded by a Bruker Tensor 27 instrument. NMR spectra were taken by a Varian 300 (300.13 MHz and 75.47 MHz for <sup>1</sup>H and <sup>13</sup>C, respectively) or 600 (599.83 MHz and 150.84 MHz for <sup>1</sup>H and <sup>13</sup>C, respectively). Atom numbering used for the NMR spectra is shown in Figure 6. Elemental analyses for

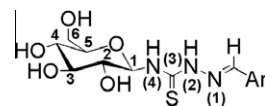
C, H, N were carried out on a Perkin–Elmer PE 2400 II instrument.

#### 3.1.2. Aldehyde 4-(per-O-acetylated-β-D-glucopyranosyl)-thiosemicarbazones 2. A general synthetic procedure

The experimental part was in accordance to that previously described by us.<sup>16</sup> A solution of the substituted benzaldehyde (2.38 mmol) in ethanol (5 mL) or 4-pyridinecarboxaldehyde in methanol was added dropwise to a solution of 4-(2,3,4,6-tetra-O-acetyl-β-D-glucopyranosyl)thiosemicarbazide (**1**) (1 g, 2.38 mmol) in ethanol (80 mL) (methanol for the pyridine analogue). After the addition of a catalytic amount of AcOH, the reaction mixture was refluxed for 4–48 h. The solution was kept in fridge overnight to form a precipitate; in some cases the solution was concentrated to the half volume at temperature below 40 °C, and then water was added to precipitate a solid. The precipitate was filtered off, washed with cold ethanol and in some cases with ether, and recrystallized from methanol or ethanol for **2pyr**. Analytical data for **2oNO2**, **2pNO2**, **2oCl**, **2mCl**, **2pCl**, **2oOH**, **2mOH**, **2pOH**, **2pOMe**, **2pCF3**, **2pMe** and **2pyr** have been reported.<sup>16</sup>

**3.1.2.1. 4-Fluoro-benzaldehyde 4-(2,3,4,6-tetra-O-acetyl-β-D-glucopyranosyl)thiosemicarbazone (2a).** Yield 40%; mp 209–212 °C (MeOH); R<sub>f</sub> (Hex/EtOAc 1:1) 0.5; [α]<sub>D</sub><sup>25</sup> –72.9 (c 1, CHCl<sub>3</sub>); IR (KBr): ν 3306 (N–H), 2975 (C–H<sub>arom</sub>), 1745 (C=O), 1553 (C=N), 1039 (C=S), 916 (1-C–H), 840 (C=S) cm<sup>–1</sup>; <sup>1</sup>H NMR (300.13 MHz, DMSO-*d*<sub>6</sub>): δ 11.93 (s, 1H, N(2)H), 8.80 (d, <sup>3</sup>J<sub>1-H,N(4)H</sub> 9.0 Hz, 1H, N(4)H), 8.07 (s, 1H, CH=N), 7.90 (dd, <sup>3</sup>J = 5.7 Hz, <sup>3</sup>J = 8.7 Hz, 2H, H<sub>arom</sub>), 7.27 (t, <sup>3</sup>J = 8.7 Hz, 2H, H<sub>arom</sub>), 5.96 (dd, <sup>3</sup>J<sub>1-H,2-H</sub> = 9.3 Hz, 1H, 1-H), 5.43–5.27 (m, 2H, 2-H, 4-H), 4.96 (t, <sup>3</sup>J = 9.6 Hz, 1H, 3-H), 4.22 (dd, <sup>3</sup>J<sub>5-H,6-H</sub> = 4.8 Hz, <sup>2</sup>J<sub>6-H,6'-H</sub> = 12.3 Hz, 1H, 6-H), 4.07 (ddd, <sup>3</sup>J<sub>4-H,5-H</sub> = 9.9 Hz, 1H, 5-H), 3.98 (dd, <sup>3</sup>J<sub>5-H,6'-H</sub> = 1.8 Hz; 1H, 6'-H), 2.00, 1.99, 1.96 and 1.93 (4 × s, 12H, CH<sub>3</sub>); <sup>13</sup>C NMR (75.47 MHz, CDCl<sub>3</sub>): δ 178.9 (C=S), 171.1, 170.7, 169.9 and 169.6 (C=O), 165.9 and 162.6 (C–F), 142.5 (CH=N), 129.7, 129.6, 129.1, 129.1, 116.3 and 116.0 (C<sub>arom</sub>), 82.3 (1-C), 73.5 (3-C), 72.6 (2-C), 70.5 (5-C), 68.3 (4-C), 61.6 (6-C), 20.8, 20.7 and 20.6 (CH<sub>3</sub>). Anal. Calcd for C<sub>22</sub>H<sub>26</sub>FN<sub>3</sub>O<sub>9</sub>S (527.52): C, 50.09; H, 4.97; N, 7.97. Found: C, 50.07; H, 5.29; N, 7.73.

**3.1.2.2. 3-Bromo-benzaldehyde 4-(2,3,4,6-tetra-O-acetyl-β-D-glucopyranosyl)thiosemicarbazone (2b).** Yield 44%; mp 183–185 °C (MeOH); R<sub>f</sub> (Hex/EtOAc 1:1) 0.5; [α]<sub>D</sub><sup>25</sup> –72.5 (c 1, CHCl<sub>3</sub>); IR (KBr): ν 3326 (N–H), 2942 (C–H<sub>arom</sub>), 1737 (C=O), 1529 (C=N), 1035 (C=S), 900 (1-C–H), 843 (C=S) cm<sup>–1</sup>; <sup>1</sup>H NMR (300.13 MHz, CDCl<sub>3</sub>): δ 10.19 (s, 1H, N(2)H), 8.34 (d, <sup>3</sup>J<sub>1-H,N(4)H</sub> = 8.7 Hz 1H, N(4)H), 7.92 (s, 1H, CH=N), 7.83 (m, 1H, H<sub>arom</sub>), 7.60 (d, <sup>3</sup>J = 7.8 Hz, 1H, H<sub>arom</sub>), 7.53 (d, <sup>3</sup>J = 7.8 Hz, 1H, H<sub>arom</sub>), 7.29 (d, <sup>3</sup>J = 7.8 Hz, 1H, H<sub>arom</sub>), 5.67 (dd, <sup>3</sup>J<sub>1-H,2-H</sub> = 9.3 Hz, 1H, 1-H), 5.41 (t, <sup>3</sup>J<sub>3-H,4-H</sub> = 9.6 Hz, 1H, 3-H), 5.21–5.09 (m, 2H, 2-H, 4-H), 4.38 (dd, <sup>3</sup>J<sub>5-H,6-H</sub> = 4.5 Hz, <sup>2</sup>J<sub>6-H,6'-H</sub> = 12.6 Hz, 1H, 6-H), 4.15 (dd, <sup>3</sup>J<sub>5-H,6'-H</sub> = 1.5 Hz, 1H, 6'-H), 3.91 (ddd, <sup>3</sup>J<sub>4-H,5-H</sub> = 10.2 Hz, 1H, 5-H), 2.08 and 2.04 and (2 × s, 12H, CH<sub>3</sub>); <sup>13</sup>C NMR (75.47 MHz, CDCl<sub>3</sub>): δ = 178.9 (C=S), 171.1, 170.7, 169.9 and 169.5 (C=O), 142.0 (CH=N), 135.0, 133.6, 130.4, 130.3, 126.4 and 123.1 (C<sub>arom</sub>), 82.3 (1-C), 73.5 (3-C), 72.5 (2-C), 70.5 (5-C), 68.4 (4-C), 61.6 (6-C), 20.8, 20.8, 20.6 and 20.6 (CH<sub>3</sub>). Anal. Calcd for C<sub>22</sub>H<sub>26</sub>BrN<sub>3</sub>O<sub>9</sub>S·3H<sub>2</sub>O (642.47): C, 41.13; H, 5.02; N, 6.54. Found: C, 41.78; H, 4.96; N, 6.21.



**Figure 6.** Atom numbering used for the NMR spectra of β-D-glucopyranosyl-thiosemicarbazones.

**3.1.2.3. 4-Bromo-benzaldehyde 4-(2,3,4,6-tetra-O-acetyl- $\beta$ -D-glucopyranosyl)thiosemicarbazone (2c)<sup>32</sup>.** Yield 64%; mp 210–212 °C (MeOH);  $R_f$  (Hex/EtOAc 1:1) 0.5;  $[\alpha]_D^{25}$  –79.8 (c 1, CHCl<sub>3</sub>); IR (KBr):  $\nu$  3134 (N–H), 2983 (C–H<sub>arom</sub>), 1741 (C=O), 1545 (C=N), 1035 (C=S), 920 (1-C–H), 822 (C=S) cm<sup>–1</sup>; <sup>1</sup>H NMR (300.13 MHz, CDCl<sub>3</sub>):  $\delta$  = 9.32 (s, 1H, N(2)H), 8.30 (d, <sup>3</sup>J<sub>1-H,N(4)H</sub> = 8.7 Hz, 1H, N(4)H), 7.69 (s, 1H, CH=N), 7.55–7.62 (m, 4H, H<sub>arom</sub>), 5.69 (dd, <sup>3</sup>J<sub>1-H,2-H</sub> = 9.3 Hz, 1H, 1-H), 5.41 (t, <sup>3</sup>J<sub>3-H,4-H</sub> = 9.6 Hz, 1H, 3-H), 5.19–5.10 (m, 2H, 2-H, 4-H), 4.39 (dd, <sup>3</sup>J<sub>5-H,6-H</sub> = 4.5 Hz, <sup>2</sup>J<sub>6-H,6'-H</sub> = 12.6 Hz, 1H, 6-H), 4.11 (dd, <sup>3</sup>J<sub>5-H,6'-H</sub> = 2.1 Hz, 1H, 6'-H), 3.90 (ddd, <sup>3</sup>J<sub>4-H,5-H</sub> = 10.2 Hz, 1H, 5-H), 2.09, 2.05, 2.04 and 2.03 (4 × s, 12H, CH<sub>3</sub>); <sup>13</sup>C NMR (75.47 MHz, CDCl<sub>3</sub>):  $\delta$  = 179.2 (C=S), 171.3, 170.7, 169.9 and 169.6 (C=O), 140.5 (CH=N), 148.8, 134.8, 132.8, 130.0, 125.0 and 122.5 (C<sub>arom</sub>), 82.4 (1-C), 73.6 (3-C), 72.5 (2-C), 70.7 (5-C), 68.4 (4-C), 61.6 (6-C), 20.8, 20.7 and 20.6 (CH<sub>3</sub>). Anal. Calcd for C<sub>22</sub>H<sub>26</sub>BrN<sub>3</sub>O<sub>9</sub>S·4H<sub>2</sub>O (660.49): C, 40.01; H, 5.19; N, 6.36. Found: C, 40.56; H, 5.68; N, 5.99.

### 3.1.3. Synthesis of aldehyde 4-( $\beta$ -D-glucopyranosyl)thiosemicarbazones 3 by deacetylation in compounds 2. A general procedure

The experimental part was in accordance to that previously described by us.<sup>16</sup> Sodium methoxide as a powder (7.5 mmol) was added to a solution of **2** (1.5 mmol) in dry methanol (20 mL). The reaction mixture was stirred at room temperature for 3 h and kept in fridge overnight. Then, the solution was neutralized with Amberlist-15 (or acetic acid for the compounds **3pCl**, **3pBr** and **3pyr**), it was filtered to remove sodium ions, and the solvent was evaporated by vacuum at a temperature below 40 °C. Purification was carried out by recrystallization. Analytical data for **3oNO2**, **3pNO2**, **3oCl**, **3mCl**, **3pCl**, **3oOH**, **3mOH**, **3pOH**, **3pOMe**, **3pCF3**, **3pMe** and **3pyr** have been reported.<sup>16</sup>

**3.1.3.1. 4-Fluoro-benzaldehyde 4-( $\beta$ -D-glucopyranosyl)thiosemicarbazone (3pF).** Yield 74%; mp 171–175 °C (decomp., MeOH/H<sub>2</sub>O 1:1);  $R_f$  (CHCl<sub>3</sub>/MeOH 5:1) 0.45;  $[\alpha]_D^{25}$  +52.9 (c 1.1, MeOH); IR (KBr):  $\nu$  3596 (OH), 2877 (C–H<sub>arom</sub>), 1545 (C=N), 1022 (C=S), 890 (1-C–H), 830 (C=S) cm<sup>–1</sup>; <sup>1</sup>H NMR (300.13 MHz, DMSO-*d*<sub>6</sub>):  $\delta$  = 11.75 (s, 1H, N(2)H), 8.60 (d, <sup>3</sup>J<sub>1-H,N(4)H</sub> = 9.0 Hz, 1H, N(4)H), 8.10 (s, 1H, CH=N), 7.96–7.91 (m, 2H, H<sub>arom</sub>), 7.29–7.23 (m, 2H, H<sub>arom</sub>), 5.38 (dd, <sup>3</sup>J<sub>1-H,2-H</sub> = 9.0 Hz, 1H, 1-H), 5.03–4.94 (m, 3H, OH), 4.50 (s, 1H, OH), 3.65 (dd, <sup>3</sup>J<sub>5-H,6-H</sub> = 5.4 Hz, <sup>2</sup>J<sub>6-H,6'-H</sub> = 11.4 Hz, 1H, 6-H), 3.53–3.14 (m, 5H, 2-H, 3-H, 4-H, 5-H, 6'-H); <sup>13</sup>C NMR (75.47 MHz, DMSO-*d*<sub>6</sub>):  $\delta$  = 178.6 (C=S), 164.8 and 161.5 (C–F), 141.8 (CH=N), 130.6, 130.6, 129.9, 129.8, 115.9 and 115.6 (C<sub>arom</sub>), 84.0 (1-C), 78.7 (3-C), 77.6 (2-C), 71.9 (5-C), 69.9 (4-C), 60.8 (6-C). Anal. Calcd for C<sub>14</sub>H<sub>18</sub>FN<sub>3</sub>O<sub>5</sub>S·5H<sub>2</sub>O (449.45): C, 37.41; H, 6.28; N, 9.35. Found: C, 37.87; H, 5.98; N, 9.56.

**3.1.3.2. 3-Bromo-benzaldehyde 4-( $\beta$ -D-glucopyranosyl)thiosemicarbazone (3mBr).** Yield 70%; mp 190–192 °C (decomp., MeOH/H<sub>2</sub>O 1:1);  $R_f$  (CHCl<sub>3</sub>/MeOH 5:1) 0.51;  $[\alpha]_D^{25}$  +49.5 (c 1, MeOH); IR (KBr):  $\nu$  3547 (OH), 2869 (C–H<sub>arom</sub>), 1533 (C=N), 1031 (C=S), 916 (1-C–H), 839 (C=S) cm<sup>–1</sup>; <sup>1</sup>H NMR (300.13 MHz, DMSO-*d*<sub>6</sub>):  $\delta$  = 11.80 (s, 1H, N(2)H), 8.72 (d, <sup>3</sup>J<sub>1-H,N(4)H</sub> = 9.0 Hz, 1H, N(4)H), 8.18 (s, 1H, H<sub>arom</sub>), 8.06 (s, 1H, CH=N), 7.76 (d, *J* = 7.5 Hz, 1H, H<sub>arom</sub>), 7.58 (d, *J* = 7.8 Hz, 1H, H<sub>arom</sub>), 7.38 (dd, *J* = 7.5 Hz, 7.8 Hz, 1H, H<sub>arom</sub>), 5.39 (dd, <sup>3</sup>J<sub>1-H,2-H</sub> = 9.3 Hz, 1H, 1-H), 5.00, 4.90, 4.49 (3 × s, 4H, OH), 3.67 (dd, <sup>3</sup>J<sub>5-H,6-H</sub> = 5.4 Hz, <sup>2</sup>J<sub>6-H,6'-H</sub> = 11.4 Hz, 1H, 6-H), 3.58–3.14 (m, 5H, 2-H, 3-H, 4-H, 5-H, 6'-H); <sup>13</sup>C NMR (75.47 MHz, DMSO-*d*<sub>6</sub>):  $\delta$  = 178.8 (C=S), 141.4 (CH=N), 136.4, 132.5, 130.7, 129.2, 127.1 and 122.3 (C<sub>arom</sub>), 84.2 (1-C), 78.7 (3-C), 77.7 (2-C), 71.8 (5-C), 69.9 (4-C), 60.9 (6-C). Anal. Calcd for C<sub>14</sub>H<sub>18</sub>BrN<sub>3</sub>O<sub>5</sub>S·3H<sub>2</sub>O (474.32): C, 35.45; H, 5.10; N, 8.86. Found: C, 35.42; H, 4.87; N, 8.45.

**3.1.3.3. 4-Bromo-benzaldehyde 4-( $\beta$ -D-glucopyranosyl)thiosemicarbazone (3pBr).** Yield 78%; mp 202–206 °C (decomp., MeOH/H<sub>2</sub>O 1:1);  $R_f$  (CHCl<sub>3</sub>/MeOH 5:1) 0.46;  $[\alpha]_D^{25}$  +86.3 (c 1, MeOH); IR (KBr):  $\nu$  3540 (OH), 2897 (C–H<sub>arom</sub>), 1553 (C=N), 1035 (C=S), 900 (1-C–H), 822 (C=S) cm<sup>–1</sup>; <sup>1</sup>H NMR (300.13 MHz, DMSO-*d*<sub>6</sub>):  $\delta$  = 11.80 (s, 1H, N(2)H), 8.62 (d, <sup>3</sup>J<sub>1-H,N(4)H</sub> = 8.7 Hz, 1H, N(4)H), 8.06 (s, 1H, CH=N), 7.81 (d, 2H, H<sub>arom</sub>), 7.61 (d, 2H, H<sub>arom</sub>), 5.36 (dd, <sup>3</sup>J<sub>1-H,2-H</sub> = 9.0 Hz, 1H, 1-H), 5.02, 4.90, 4.49 (3 × s, 4H, OH), 3.64 (dd, <sup>3</sup>J<sub>5-H,6-H</sub> = 5.4 Hz, <sup>2</sup>J<sub>6-H,6'-H</sub> = 11.4 Hz, 1H, 6-H), 3.52–3.14 (m, 5H, 2-H, 3-H, 4-H, 5-H, 6'-H); <sup>13</sup>C NMR (75.47 MHz, DMSO-*d*<sub>6</sub>):  $\delta$  = 178.7 (C=S), 141.8 (CH=N), 133.3, 131.7, 129.5 and 123.3 (C<sub>arom</sub>), 84.1 (1-C), 78.7 (3-C), 77.6 (2-C), 72.0 (5-C), 69.9 (4-C), 60.9 (6-C). Anal. Calcd for C<sub>14</sub>H<sub>18</sub>BrN<sub>3</sub>O<sub>5</sub>S (420.28): C, 40.01; H, 4.32; N, 10.00. Found: C, 39.78; H, 4.85; N, 10.03.

## 3.2. Enzyme preparation and kinetic experiments

Glycogen phosphorylase (GPb) was isolated from rabbit skeletal muscle and purified as described previously.<sup>33</sup> Kinetic studies were performed in the direction of glycogen synthesis in the presence of various concentrations of inhibitors. All kinetic experiments were carried out in the presence of 30 mM imidazole/HCl buffer 60 mM KCl, 0.6 mM EDTA, and 0.6 mM dithiothreitol (pH 6.8), 0.2% (w/v) glycogen, 1 mM AMP and various concentrations of Glc-1-P. Experiments were performed in the presence of 1% v/v DMSO and *K<sub>m</sub>* of the enzyme for Glc-1-P was 2.2–3.0 mM. Enzyme activity was measured at pH 6.8 by the release of inorganic phosphate as described previously.<sup>34</sup>

## 3.3. X-ray crystallography

Crystallographic binding studies were performed by diffusion of a solution of  $\beta$ -D-glucopyranosyl thiosemicarbazones in the crystallization media with 20% v/v of DMSO into preformed GPb crystals, grown in the tetragonal lattice, space group *P*<sub>4</sub><sub>3</sub><sub>2</sub><sub>1</sub><sub>2</sub>, as previously described.<sup>35</sup> Experimental conditions for the formation of the GPb-inhibitor complexes were as follows: 20 mM of **3pF** (13 h), or **3pBr** (16 h), or **3oCl** (11.5 h), or **3mCl** (16 h), or **3pCl** (21 h), or **3oOH** (21 h), or **3mOH** (3.5 h), or **3pOH** (21 h), or **3pMe** (3.5 h), or **3pyr** (7 h), 10 mM **3pCF3** (7 h), 5 mM **3oNO2** (18 h), 6.7 mM **3pNO2** (3 h), or **3pOMe** (3 h), and 10 mM **3mBr** (7 h). Diffraction data were collected at EMBL-Hamburg outstation (Beamline X13), Daresbury Synchrotron Laboratory, UK (Beamline PX 10.1) and Max-Lab, Lund (Beamline ID9111-2). Crystal orientation, integration of reflections, inter-frame scaling, partial reflection summation, data reduction and post-refinement were all performed using the HKL program suite.<sup>36</sup>

Crystallographic refinement of the complexes was performed by maximum-likelihood methods using REFMAC.<sup>37</sup> The starting model employed for the refinement of the complexes was the structure of the native T state GPb complex determined at 1.9 Å resolution (Leonidas et al., unpublished results). Inhibitor molecules were modeled using the Dundee PRODRG server (<http://dav.apc1.bioch.dundee.ac.uk/programs/prodrgr/>), they were included in the refinement procedure during its final stages and they were fitted to the electron density maps after adjustment of their torsion angles. Alternate cycles of manual rebuilding with 'COOT' and refinement with REFMAC improved the quality of the models. The stereochemistry of the protein residues was validated by PROCHECK.<sup>38</sup> Hydrogen bonds and van der Waals interactions were calculated with the program CONTACT as implemented in CCP4<sup>39</sup> applying a distance cut off 3.3 Å and 4.0 Å, respectively. Protein structures were superimposed using LSQKAB.<sup>39</sup> The figures were prepared with the programs MOLSCRIPT,<sup>40</sup> or Bobscript<sup>41</sup> and rendered with Raster3D.<sup>42</sup> The coordinates of the new structures have been deposited with the RCSB Protein Data Bank (<http://>



[www.rcsb.org/pdb](http://www.rcsb.org/pdb)) with codes with codes 3MQF (**3pF**), 3MTA (**3mBr**), 3MT7 (**3pBr**), 3MS7 (**3oCl**), 3MTB (**3mCl**), 3MT8 (**3pCl**), 3MS4 (**3pCF3**), 3MSC (**3oNO2**), 3MT9 (**3pNO2**), 3NC4 (**3oOH**), 3MRV (**3mOH**), 3MTD (**3pOH**), 3MRX (**3pOMe**), 3MS2 (**3pMe**) and 3MRT (**3pyr**).

## Acknowledgements

This work was supported by the EU Marie Curie Early Stage Training (EST) contract no. MEST-CT-020575 and by the Commission of the European Communities—under the FP7 ‘SP4-Capacities Coordination and Support Action, Support Actions’ EUROSTRUCT project (CSA-SA\_FP7-REGPOT-2008-1 Grant Agreement No. 230146). This work was also supported by grants from European Community—Research Infrastructure Action under the FP6 ‘Structuring the European Research Area’ Programme (through the Integrated Infrastructure Initiative ‘Integrating Activity on Synchrotron and Free Electron Laser Science’) for work at the Synchrotron Radiation Source MAX-lab, Lund, Sweden, and EMBL-Hamburg Outstation, Germany.

## Supplementary data

Supplementary data associated with this article can be found, in the online version, at [doi:10.1016/j.bmc.2010.09.039](https://doi.org/10.1016/j.bmc.2010.09.039).

## References and notes

- Green, A.; Christian Hirsch, N.; Pramming, S. K. *Diabetes Metab. Res. Rev.* **2003**, *19*, 3.
- Aiston, S.; Andersen, B.; Agius, L. *Diabetes* **2003**, *52*, 1333.
- Aiston, S.; Coghlan, M. P.; Agius, L. *Eur. J. Biochem.* **2003**, *270*, 2773.
- Oikonomakos, N. G. *Curr. Protein Pept. Sci.* **2002**, *3*, 561.
- Oikonomakos, N. G.; Somsak, L. *Curr. Opin. Invest. Drugs* **2008**, *9*, 379.
- Treadway, J. L.; Mendys, P.; Hoover, D. J. *Expert Opin. Invest. Drugs* **2001**, *10*, 439.
- Baker, D. J.; Timmons, J. A.; Greenhaff, P. L. *Diabetes* **2005**, *54*, 2453.
- Somsak, L.; Czifrak, K.; Toth, M.; Bokor, E.; Chrysina, E. D.; Alexacou, K. M.; Hayes, J. M.; Tiraidis, C.; Lazoura, E.; Leonidas, D. D.; Zographos, S. E.; Oikonomakos, N. G. *Curr. Med. Chem.* **2008**, *15*, 2933.
- Oikonomakos, N. G.; Skamnaki, V. T.; Tsitsanou, K. E.; Gavalas, N. G.; Johnson, L. N. *Structure* **2000**, *8*, 575.
- Rath, V. L.; Ammirati, M.; Danley, D. E.; Ekstrom, J. L.; Gibbs, E. M.; Hynes, T. R.; Mathiowetz, A. M.; McPherson, R. K.; Olson, T. V.; Treadway, J. L.; Hoover, D. J. *Chem. Biol.* **2000**, *7*, 677.
- Oikonomakos, N. G.; Kosmopoulou, M.; Zographos, S. E.; Leonidas, D. D.; Chrysina, E. D.; Somsak, L.; Nagy, V.; Praly, J. P.; Docsa, T.; Toth, B.; Gergely, P. *Eur. J. Biochem.* **2002**, *269*, 1684.
- Beraldo, H.; Gambino, D. *Mini-Rev. Med. Chem.* **2004**, *4*, 31.
- Belicchi-Ferrari, M.; Bisceglie, F.; Casoli, C.; Durot, S.; Morgenstern-Badarau, I.; Pelosi, G.; Pilotti, E.; Pinelli, S.; Tarasconi, P. *J. Med. Chem.* **2005**, *48*, 1671.
- Kovala-Demertzi, D.; Papageorgiou, A.; Papathanasis, L.; Alexandratos, A.; Dalezis, P.; Miller, J. R.; Demertzis, M. A. *Eur. J. Med. Chem.* **2009**, *44*, 1296.
- Kovala-Demertzi, D.; Yadav, P. N.; Wiecek, J.; Skoulika, S.; Varadinova, T.; Demertzis, M. A. *J. Inorg. Biochem.* **2006**, *100*, 1558.
- Tenchiu (Deleanu), A.-C.; Kostas, I. D.; Kovala-Demertzi, D.; Terzis, A. *Carbohydr. Res.* **2009**, *344*, 1352.
- Zhang, S. S.; Ye, S. J.; Li, X. M.; Gu, S. S.; Liu, Q. *Chem. Res. Chin. U* **2005**, *21*, 545.
- Ghosh, S.; Misra, A. K.; Bhatia, G.; Khan, M. M.; Khanna, A. K. *Bioorg. Med. Chem. Lett.* **2009**, *19*, 386.
- Zemplén, G.; Gerecs, A.; Hadácsy, I. *Ber. Dtsch. Chem. Ges.* **1936**, *69*, 1827.
- Johnson, L. N. *FASEB J.* **1992**, *6*, 2274.
- O'Reilly, M.; Watson, K. A.; Schinzel, R.; Palm, D.; Johnson, L. N. *Nat. Struct. Biol.* **1997**, *4*, 405.
- Watson, K. A.; Schinzel, R.; Palm, D.; Johnson, L. N. *EMBO J.* **1997**, *16*, 1.
- Barford, D.; Johnson, L. N. *Nature* **1989**, *340*, 609.
- Martin, J. L.; Veluraja, K.; Ross, K.; Johnson, L. N.; Fleet, G. W. J.; Ramsden, N. G.; Bruce, I.; Orchard, M. G.; Oikonomakos, N. G.; Papageorgiou, A. C.; Leonidas, D. D.; Tsitoura, H. S. *Biochemistry (USA)* **1991**, *30*, 10101.
- Alexacou, K. M.; Hayes, J. M.; Tiraidis, C.; Zographos, S. E.; Leonidas, D. D.; Chrysina, E. D.; Archontis, G.; Oikonomakos, N. G.; Paul, J. V.; Varghese, B.; Loganathan, D. *Proteins* **2008**, *71*, 1307.
- Howard, J. A. K.; Hoy, V. J.; OHagan, D.; Smith, G. T. *Tetrahedron* **1996**, *52*, 12613.
- Tsirkone, V. G.; Tsoukala, E.; Lamprakis, C.; Manta, S.; Hayes, J. M.; Skamnaki, V. T.; Drakou, C.; Zographos, S. E.; Komiotis, D.; Leonidas, D. D. *Bioorg. Med. Chem.* **2010**, *18*, 3413.
- Auffinger, P.; Hays, F. A.; Westhof, E.; Ho, P. S. *Proc. Natl. Acad. Sci. USA* **2004**, *101*, 16789.
- Politzer, P.; Lane, P.; Concha, M. C.; Ma, Y. G.; Murray, J. S. *J. Mol. Model.* **2007**, *13*, 305.
- Lindhorst, T. K.; Kieburg, C. *Synthesis-Stuttgart* **1995**, 1228.
- Cateni, F.; Bonivento, P.; Procida, G.; Zaccogna, M.; Favretto, L. G.; Scialino, G.; Banfi, E. *Bioorg. Med. Chem.* **2007**, *15*, 815.
- Although it is a known compound, full analytical data is not accessible: Cao, K.; Wang, Z.; Zhao, X. *Shiyou Daxue Xuebao, Ziran Kexueban* **2004**, *28*, 100.
- Melpidou, A. E.; Oikonomakos, N. G. *FEBS Lett.* **1983**, *154*, 105.
- Saheki, S.; Takeda, A.; Shimazu, T. *Anal. Biochem.* **1985**, *148*, 277.
- Oikonomakos, N. G.; Melpidou, A. E.; Johnson, L. N. *Biochim. Biophys. Acta* **1985**, *832*, 248.
- Otwinowski, Z.; Minor, W. In *Methods Enzymology*; Carter, C. W. J., Sweet, R. M., Eds.; Academic Press: New York, 1997; Vol. 276, p 307.
- Murshudov, G. N.; Vagin, A. A.; Dodson, E. J. *Acta Crystallogr., Sect. D* **1997**, *53*, 240.
- Laskowski, R. A.; MacArthur, M. W.; Moss, D. S.; Thornton, J. M. *J. Appl. Crystallogr.* **1993**, *26*, 283.
- CCP4 *Acta Crystallogr., Sect. D* **1994**, *50*, 760.
- Kraulis, P. J. *J. Appl. Crystallogr.* **1991**, *24*, 946.
- Esnouf, R. M. *J. Mol. Graphics Modell.* **1997**, *15*, 132.
- Merritt, E. A.; Bacon, D. J. *Macromol. Crystallogr.* **1997**, *B277*, 505.